Contents lists available at ScienceDirect

Translational Oncology

Original Research

LCMT1 indicates poor prognosis and is essential for cell proliferation in hepatocellular carcinoma

Ning Zhang [a,b,1], Cailing Lu [a,b,1], Jiao Mo [a,b,1], Xinhang Wang [a,b,c], Simi Liao [a,b],
Ningjing Liang [a,b], Mei Feng [c], Tingting Tang [a,b], Yijie Wu [a,b], Yunqing Li [a,b], Chunhua Lan [c],
Chengying Chen [c], Qianqian Shi [a,b], Lancheng Wei [a,b], Zhijian Zheng [a,b], Yu Lei [a,b],
Zhiming Zhang [d], Shen Tang [c,*], Xiyi Li [a,b,**]

[a] *School of Public Health, Guangxi Medical University, Nanning, China*
[b] *Guangxi Colleges and University Key Laboratory of Prevention and Control of Highly Prevalent Diseases, Guangxi Medical University, China*
[c] *School of Basic Medical Sciences, Guangxi Medical University, Nanning, China*
[d] *Guangxi Medical University Affiliated Tumor Hospital, China*

ARTICLE INFO

ABSTRACT

Background: Hepatocellular carcinoma (HCC) is one of the most malignant type of cancers. Leuci carboxyl methyltransferase 1 (LCMT1) is a protein methyltransferase that plays an improtant regulatory role in both normal and cancer cells. The aim of this study is to evaluate the expression pattern and clinical significance of LCMT1 in HCC.

Methods: The expression pattern and clinical relevance of LCMT1 were determined using the Gene Expression Omnibus (GEO) database, the Cancer Genome Atlas (TCGA) program, and our datasets. Gain-of-function and loss-of-function studies were employed to investigate the cellular functions of LCMT1 *in vitro* and *in vivo*. Quantitative real-time polymerase chain reaction (RT-PCR) analysis, western blotting, enzymatic assay, and high-performance liquid chromatography were applied to reveal the underlying molecular functions of LCMT1.

Results: LCMT1 was upregulated in human HCC tissues, which correlated with a "poor" prognosis. The siRNA-mediated knockdown of LCMT1 inhibited glycolysis, promoted mitochondrial dysfunction, and increased intracellular pyruvate levels by upregulating the expression of alani-neglyoxylate and serine-pyruvate amino-transferase (AGXT). The overexpression of LCMT1 showed the opposite results. Silencing LCMT1 inhibited the proliferation of HCC cells *in vitro* and reduced the growth of tumor xenografts in mice. Mechanistically, the effect of LCMT1 on the proliferation of HCC cells was partially dependent on PP2A.

Conclusions: Our data revealed a novel role of LCMT1 in the proliferation of HCC cells. In addition, we provided novel insights into the effects of glycolysis-related pathways on the LCMT1regulated progression of HCC, suggesting LCMT1 as a novel therapeutic target for HCC therapy.

Introduction

Throughout the world, liver cancer is the sixth most common malignancy and the third leading cause of deaths from cancer. Hepatocellular carcinoma (HCC), which is the primary type of liver cancer, accounts for 90% of liver-cancer cases [1,2]. The cure rate of resecting early-stage HCC by radical hepatectomy can reach 70–80% [3]. Unfortunately, in most HCC patients, when it is diagnosed, the cancer has been in an advanced stage. Therefore, chemical therapy is the only therapy for those patients [1,3]. For more than a decade, targeted-therapy drugs, such as sorafenib, have been the first-line drugs for treating advanced HCC. However, the treatment for advanced HCC is limited by multiple targets, single-drug use, and long-term drug resistance [4]. Hence, in recent years, there have been fast developments in targeted-therapy drugs and immunotherapy. Finding novel molecular targets is imperative to improve the therapeutic outcomes of the treatments for HCC [5–7].

* Corresponding author.
** Corresponding author at: School of Public Health, Guangxi Medical University, Nanning, China.
E-mail addresses: zn11025@163.com (S. Tang), xiyi.li2017@hotmail.com (X. Li).
[1] First author

Leucine carboxyl methyltransferase 1 (LCMT1) is a 38-kDa protein methyltransferase consisted of 338 amino acids. It is found in nearly all groups of eukaryotes and is conserved in yeast, mice, and humans. LCMT1 is expressed in many tissues of the body, but the level of its expression varies greatly among tissues. In humans and rodents, LCMT1 is highly expressed in the brain, testis, and placenta, but the expression of LCMT1 in the liver is low [8]. LCMT1 belongs to the S-adenosyl-L-methionine (SAM)-dependent methyltransferase family, which catalyzes the transfer of methyl groups from SAM to an acceptor molecule. Three protein phosphatases have been identified as the acceptors of the methyl groups. Protein phosphatase 2A (PP2A) was the first identified and is the most explored acceptor of the methyl groups. LCMT1 is responsible for methylating the carboxyl group of the C-terminal leucine of the catalytic subunit of PP2A (PP2Ac). PP2Ac regulates PP2A activity and tissue specificity [9]. Recently, PP4 and PP6, which are the members of the PP2A subfamily, have been identified as the other two protein phosphatases. PP4 and PP6, which are serine/threonine protein phosphatases, have conserved C termini and conserved active-site residues [10]. Therefore, it is likely that LCMT1 regulates the functions of these phosphatases in cellular processes (such as cell growth and proliferation) by regulating the formation of the methylation-dependent complexes of the phosphatases.

To date, the associations between LCMT1 and neurodegenerative disorders (such as Alzheimer's disease [11], Parkinson [12], and manganese-related neurotoxicity [13]) have been proven. Neurodegenerative damage decreases the level of LCMT1 in the brain [14]. LCMT1 knockdown accelerates brain injuries, and LCMT1 overexpression reverses the damage [15,16]. Therefore, LCMT1 may support neurocytes to maintain the normal brain function. The associations between LCMT1 and cancers are limited and indecisive. According to the present knowledge, the methylation of PP2Ac promotes the assembly of substrate-specific PP2A trimeric holoenzymes. The holoenzymes, in particular those with the PPP2R2 and PPP2R5 regulatory B-type subunits, possess tumor-suppressive functions by suppressing the MAP kinase and Akt pathways [17]. Moreover, the methylation of PP4c is required for the formation of the PP4R1/PP4c complex that negatively regulates the NF-κB pathway [18]. Thus, LCMT1 is expected to be a tumor suppressor because it blocks the oncogenic transformation of transfected HEK cells by inactivating the Akt pathway [19]. In glioblastoma, the downregulation of nicotinamide N-methyltransferase (NNMT), a methyltransferase that catalyzes the transfer of a methyl group from SAM to nicotinamide, upregulates the expression of LCMT1 and inhibits the activity of oncogenic kinases [20]. The evidence supports the above hypothesis. However, in cervical and colon cancer cells, the knockdown of LCMT1 induces cell death [17,21], which indicates that LCMT1 plays a crucial role in the survival of tumor cells. These contradictory results imply that the effects of LCMT1 on different types of cancer are tissue specific. The role of LCMT1 in the development of HCC is elusive and worth exploring. Therefore, this study was designed to evaluate the clinical significance of LCMT1 in HCC.

Materials and methods

Bioinformatic analysis based on public clinical databases

Gene Expression Profiling Interactive Analysis (GEPIA, http://gepia.cancer-pku.cn/), which is an open-source genetic database, was used to analyze the overall survival (OS) and disease-free survival (DFS) of HCC patients and the expression levels of LCMT1 in the patients. HCC expression datasets including RNA-seq data and the corresponding clinical information were extracted from GEPIA. The median risk score was used as the cut-off value for grouping into a high-risk group and a low-risk group. Then, the relationships among the LCMT1 expression level, clinical information, and survival status were analyzed.

Extraction of microarray data from the Gene expression omnibus (GEO) database

The microarray data on HCC published from 2020 onwards were obtained from the GEO database (http://www.ncbi.nlm.nih.gov/geo/), which is a public repository for functional genomic datasets. The keywords used for finding the microarray data in the GEO database were "liver/hepatocellular/hepatic" and "cancer/tumor/carcinoma". The "Organism" was restricted to "*Homo sapiens*", and the "Study type" was restricted to "mRNA expression profiling by array". The inclusion criteria were as follows: (1) the files contained data for normal (nontumorous) tissues and HCC tissues, (2) each group contained more than 5 cases, and (3) the microarray data on the expression of LCMT1 were limited to a close range and were directly available for analysis. Array-based and sequence-based data were obtained from different platforms. Then, a meta-analysis was performed on the GEO datasets.

Samples of human livers with HCC

HCC tissues and the adjacent nontumorous tissues were collected from HCC patients who underwent resections on the tumor at The Affiliated Tumor Hospital of Guangxi Medical University (Nanning, China) between 2019 and 2020. The human study was approved by the Ethics Committee of Guangxi Medical University (No. 20210144).

Cell lines

Human HCC cell lines (HepG2, Huh7, and Hep3B) were obtained from the National Collection of Authenticated Cell Cultures (Shanghai, China). The HCC cells were cultured in Minimum Essential Media (MEM) containing 10% of fetal bovine serum and 1% of a penicillin–streptomycin mixture according to the ATCC Animal Cell Culture Guide. All cultures were maintained under a 5% CO_2 environment and humidified conditions in a 37 °C cell-culture incubator.

Transfection of siRNA

Small interfering RNA (siRNA) against human LCMT1 and siRNA against AGXT were synthesized by Gene Pharma (Suzhou, China). The target sequences were as follows: the sense sequence of siRNA-LCMT1 (siLCMT1) was 5'-GGCAUGGAUACCACCUUCGGAGAU-3', the sense sequence of siRNA-AGXT (siAGXT) was 5'-GCUACGUCAUAGACCA-CUUTT-3', the antisense sequence of siAGXT was 5'-AAGUGGUCUAU-GACGUAGCTT-3', the sense sequence of siRNA control (siCtrl) was 5'-GCGACGAUCUGCCUAAGAUdTdT-3', and the antisense sequence of siCtrl was 5'-AUCUUAGGCAGAUCGUCGCdTdT-3'. The siRNA was transfected into HepG2 and Huh7 cells by the Lipofectamine 3000 RNAiMAX transfection reagent (Thermo Fisher Scientific, USA) according to the manufacturer's instructions. After being transfected with the siRNA, the cells were grown for 48 h. Then, the cells were used for follow-up studies.

Plasmid construction and genetic transfection

Recombinant plasmid LCMT1-pcDNA3.0 was constructed according to our previous report [22]. The recombinant plasmid was transfected into the Hep3B cell line using Lipofectamine 3000 RNAiMAX according to the procedure recommended by the manufacturer. Stably transfected cells were selected by incubating the transfected cells with G418 (800 mg/mL) for about 20 days. The stably transfected cells were verified with RT-PCR and western blotting. Then, the cells were grown to generate frozen stocks of early-passage cells. All successive experiments were performed with the early-passage cells.

In-vivo tumor-suppressive activity of LCMT1 siRNA treatment

Male nude mice (4–5 weeks old) were purchased from Guangxi Medical University Laboratory Animal Center and maintained under specific-pathogen-free (SPF) conditions. A total of 5×10^6 Huh7 cells were injected into the subcutaneous tissue of each mouse. The length and width of each tumor were measured with a micrometer caliper every other day, and the volume of the tumor was calculated using the following formula: volume $= 0.5 \times \text{width}^2 \times \text{length}$. When tumors developed in the mice (the volume of the tumors was 80–100 mm³), the mice were randomly divided into two treatment groups (five mice in each group). For 10 days, siRNA of LCMT1 (20 μg of siRNA per injection) was injected into the tumors directly every two days. At the end of the experiment, the weight of the tumors was measured, and the tumors were stored in 4% polyoxymethylene for H&E staining. All experimental treatments were undertaken in accordance with the National Institutes of Health Guide for the Care and Use of Laboratory Animals. The experiments were approved by the Animal Care & Welfare Committee of Guangxi Medical University (Nanning, China).

Cell proliferation assays and cell growth curves

After transfection for 48 h, transfected HepG2 and transfected Huh7 cells (1×10^4 cells/well) were seeded in 96-well plates, and the proliferation rates of the cells were detected by Cell Counting Kit-8 (CCK-8) from Dojindo Molecular Technologies, Inc. Hep3B cells were grown for 2 days, and the viability of the cells was detected on the second day. Thereafter, the viability of the cells was detected every other day for 10 days (a total of five cell-viability measurements). Growth media were replaced every two days to prevent nutrient depletion. The cell proliferation rate and cell proliferation curve were determined by measuring the optical density (OD) at 450 nm.

Measurement of the level of EdU incorporated into cells

EdU staining was performed using EdU Assay Kits (APExBIO, USA). Cells and 20 μM of 5-ethynyl-2'-deoxyuridine (EdU) were incubated for 8 h according to the manufacturer's instructions. Then, the staining reagent was captured using fluorescence microscopy.

RNA isolation and quantitative real-time PCR (RT-PCR) analysis

Total RNA was isolated from cells and tissues using the TRIzol Reagent (Tiangen, China). The quality and concentration of the RNA were determined by spectrophotometry. cDNA was prepared using M-MLV reverse transcriptase (Takara, Japan). RT-PCR was performed using a LightCycler 480 Real-Time PCR System (Roche, Switzerland) and SYBR Premix Dimer Eraser™ (TakaraBio, Japan). The sequences of the target genes are shown in Supplementary Table. The relative abundance of the target genes was normalized to the abundance of β-actin and was estimated using the $2^{-\Delta CT}$ formula.

Protein extraction and western blotting

Western blotting was performed according to standard protocols. Briefly, cells and tissues were lysed in RIPA Buffer (Beyotime, China), and the protein concentration was determined by the BCA Protein Assay Kit (Takara, Japan). The protein lysates were subjected to SDS-PAGE analysis using 10% SDS-PAGE gels, followed by the transfer of the proteins to PVDF membranes (Millipore, USA). For 30 min, the membranes were placed in TBST containing 5% dry milk. Then, the membranes and the specific primary antibodies were incubated at 4 °C overnight. Afterwards, the membranes and the secondary antibody were incubated at 37 °C for 2 h. The protein signals were detected by the enhanced chemiluminescence reagent (Thermo Fisher Scientific, USA) and quantified using iBright Analysis Software. The profiles and manufacturers of the primary antibodies tested in this study were as follows: 1:500 LCMT1 (D-10) from Santa Cruz Biotechnology, 1:1000 PME-1 (A10) from Santa Cruz Biotechnology, 1:500 anti-demethylated-PP2A-C from Santa Cruz Biotechnology, 1:500 anti-PP2A alpha + beta from Abcam, and 1:4000 α-tubulin from Beyotime.

Measurement of the uptake of glucose

HepG2 and Huh7 cells transfected with siLCMT1 were cultured for 48 h in wells, and Hep3B cells in which LCMT1 was overexpressed were cultured for 24 h. The media were collected, and the cells were removed from the media by centrifugation. Then, the glucose content was measured by the Glucose Uptake Assay Kit (Solarbio, China) according to the manufacturer's instructions. The level of glucose in each medium was determined by measuring the OD at 525 nm.

Measurement of the level of lactate, level of pyruvate, activity of pyruvate kinase, and activity of lactate dehydrogenase

The medium was removed, and the transfected cells were washed three times with phosphate-buffered saline (PBS). Then, a lysis buffer was added to the cells, and the cells were scraped on ice using a cell scraper. Every 3 seconds, the cells were lysed by ultrasonic degradation (a 30% amplitude). The ultrasonic degradation was repeated 30 times. Each extract was centrifuged at $8000 \times g$ and 4 °C for 10 min. The lactate (LA) content and the pyruvate (PA) content were detected by the Lactate Assay Kit (Solarbio, China) and the Pyruvic Acid Assay Kit (Solarbio, China), respectively, according to the manufacturer's instructions. The activity of pyruvate kinase (PK) and the activity of lactate dehydrogenase (LDH) were detected by the Pyruvate Kinase Activity Assay Kit (Solarbio, China) and the Lactate Dehydrogenase Activity Assay Kit (Solarbio, China), respectively, according to the manufacturer's instructions.

Measurement of intracellular levels of reactive oxygen species (ROS)

Intracellular ROS levels were quantified with 2',7'-dichloro-fluorescein-diacetate (DCFH-DA) from Beyotime (China). DCFH-DA is easily oxidized by intracellular ROS to fluorescent dichlorofluorescein (DCF). The cells in the wells were gently washed twice with PBS. Then, the cells and 20 μM of DCFH-DA were incubated at 37 °C for 20 min. The dye was removed and replaced with fresh PBS. The fluorescence emitted by the cells was measured immediately by a fluorescence spectrophotometer (Spark 10M, Tecan, Switzerland). The λ_{ex} was 488 nm, and the λ_{em} was 525 nm.

Measurement of mitochondrial membrane potential (MMP)

Changes in MMP were captured by the JC-1 fluorescent probe (Beyotime, China). JC-1 has unique labeling features. Under a high MMP, JC-1 forms multimeric aggregates and emits red fluorescence with a wavelength of 525–590 nm. Under a low MMP, JC-1 is a monomer that emits green fluorescence with a wavelength of 490–530 nm. Briefly, in the culture medium, cells and JC-1 (10 μM) were incubated at 37 °C for 20 min. Then, the cells were washed and suspended in JC-1 staining buffer ($1 \times$) two to three times. After the fluorescent labelling, the cells were viewed by an inverted fluorescence microscope, and the intensity of the fluorescence was measured with a multimode reader (Spark 10M, Tecan, Switzerland). The ratio of the intensity of the green fluorescence to the intensity of the red fluorescence revealed the change in MMP.

Measurement of the mitochondrial redox capacity

The resazurin sodium salt (RSS) is a redox indicator that can be used to evaluate metabolic function. RSS can be reduced by cytochromes, FMNH2, FADH, NADH, and NADPH, which are involved in the electron

transport chain [23]. Cells and 1% of RSS, which diluted with serum-free MEM, were incubated for 2 h. The OD at 560 nm and OD at 590 nm were measured with a multifunctional microplate reader.

Quantification of amino acids by high-performance liquid chromatography

The amino acids secreted in the culture medium were determined by high-performance liquid chromatography (HPLC) with an ultraviolet (UV) detector. The medium was diluted with a 10% solution of 5-sulfo-salicylic acid dihydrate. The volume of the solution added to the medium was equal to the volume of the medium. Then, all samples were clarified by centrifugation at 10,000 g and 4 °C for 10 min. The supernatant was removed with an automatic injection bottle and passed through an organic phase filter (the pore size of the filter was 0.22 μm, and the diameter of the filter was 13 mm). The supernatant was tested within 24 h after obtainment. The content of each amino acid was quantified with an external standard method and calculated using an S433D UPLC amino acid analyzer (Sykam, Germany). The area under each peak was quantified using Clarity Software.

Detection of cellular ATP levels

Cellular ATP levels were measured using an ATP assay kit based on firefly luciferase (Beyotime, China) according to the manufacturer's instructions. Briefly, cells were lysed and centrifuged at 12,000 g for 5 min. In a 96-well plate, 50 μL of each supernatant was mixed with 50 μL of the ATP working solution. The luminescence intensity was linearly related to the ATP concentration and was measured using a monochromator-based microplate reader (Spark 10M, Tecan, Switzerland).

Statistical analysis

Each molecular study and each in-*vivo* experiment were repeated independently at least three times. All continuous variables were reported in terms of means ± standard deviations and were analyzed using the student's *t*-test. Chi-square test was used for evaluating the relationship between two groups. All analyses were performed by SPSS 17.0 statistical software (Chicago, USA). The statistical significance was defined as $p < 0.05$. *, **, and *** stood for $p < 0.05$, $p < 0.01$, and $p < 0.001$, respectively.

Results

LCMT1 was upregulated in human HCC tissue and was a "poor" prognostic factor

To explore the role of LCMT1 in the progression of human HCC, firstly we examined the levels of LCMT1 expression in 34 pairs of human primary liver tumors and adjacent normal liver tissues. The results obtained by western blotting and RT-PCR showed that the levels of LCMT1 expression in HCC tissues were higher than those of LCMT1 expression in adjacent nontumorous liver tissues (Fig. 1A and B). These results were supported by the RNA-seq data on the expression levels of LCMT1 in 50 normal liver specimens and 369 HCC (known as LIHC) patients (Fig. 1C). The data were extracted from The Cancer Genome Atlas (TGCA). Secondly, to confirm the level of LCMT1 expression in HCC, we included six GEO datasets (GSE29721, GSE50579, GSE57555, GSE101685, GSE101728, and GSE121248) in our study. The normalized expression levels of LCMT1 in nontumorous tissues and HCC tissues are shown in Fig. 1D and Table 1. The data were obtained from the GEO datasets. Furthermore, to draw a credible conclusion and to reduce the effect of the small sample size of each dataset, a meta-analysis was carried out under the fixed-effect model (Fig. 1E). No significant heterogeneity existed among six trials ($p = 0.14$, $I^2 = 39\%$). The combined effect indicated that the expression levels of LCMT1 in HCC tissues were higher

than those of LCMT1 in normal tissues (SMD = 1.21, 95% CI [0.91, 1.50]). No significant publication bias was observed (Begg's test, $p = 0.602$; Fig. 1F) among the datasets. In addition, we investigated the relationships between the expression of LCMT1 and clinical features of HCC patients. High levels of LCMT1 expression were noticed in high stages of the tumor (Fig. 1G). And, The results showed that the expression level of LCMT1 was significantly associated with the Asian race ($p = 0.008$), tumor histologic grade ($p = 0.006$), tumor size ($p = 0.016$), and family history ($p = 0.010$). However, the expression level of LCMT1 was not significantly associated with other clinicopathological characteristics such as age, gender, alcohol consumption, HBV infection, and vascular invasion ($p > 0.050$, Table 2), Finally, Kaplan–Meier survival curves showed that high LCMT1 expression was significantly associated with the low OS and DFS of the HCC patients (Fig. 1H). Together, these results indicate that LCMT1 is upregulated in HCC patients and is a predictor for a poor prognosis.

LCMT1 drove metabolic reprogramming of glycolysis in HCC cells

Metabolic reprogramming is a hallmark of malignancy. Cancer cell proliferation is a metabolically demanding process. It requires a high rate of glycolysis to generate a large amount of ATP and to support the Warburg effect [24,25]. ATP is an energy source that connects catabolism and anabolism. It is required to support cellular processes such as growth, proliferation, protein transport, and post-translational modification. ATP is especially required by cancer cells. We measured a series of metabolic parameters in HepG2 and Huh7 cells in which LCMT1 was knocked down and in Hep3B cells in which LCMT1 was overexpressed. The transfection rates of siRNA into HepG2 and Huh7 cells were demonstrated by florescence intensities, which constantly showed transfection rates above 80%. Results of western blotting showed 80% and 70% reductions in the expression levels of LCMT1 in HepG2 cells and Huh7 cells, respectively (Supplementary Fig. 2A and Supplementary Fig. 2B). In Hep3B cells, the expression of LCMT1 increased by 60% (Supplementary Fig. 2C). Using these models, firstly, we examined the levels of ATP at different expression levels of LCMT1. The results showed that the production of ATP in LCMT1-silenced HepG2 and LCMT1-silenced Huh7 cells reduced significantly, and the production of ATP in LCMT1-overexpressed Hep3B cells increased (Fig. 2A). Secondly, we explored the glycolysis-associated metabolites and enzymatic activity. As shown in Fig. 2B, in HepG2 and Huh7 cells, silencing LCMT1 reduces the uptake of glucose, production of intracellular lactate, activity of PK, and activity of LDH. As expected, in Hep3B cells, the overexpression of LCMT1 increased the uptake of glucose, production of lactate, activity of PK, and activity of LDH (Fig. 2C). Thirdly, the expression levels of some key glycolytic genes in LCMT1-silenced cells and LCMT1-overexpressed cells were detected. In Huh7 and HepG2 cells, silencing LCMT1 reduced the mRNA levels of GLUT1, HK2, PFK2, and MCT4 (Fig. 2D). In Hep3B cells, the overexpression of LCMT1 increased the mRNA levels of GLUT1, HK2, PFK2, and MCT4 (Fig. 2E). Finally, to verify the relationships between LCMT1 and the glycolytic genes, we used GEPIA to analyze the correlations between the expression levels of LCMT1 in HCC specimens and the expression levels of the glycolytic genes in the specimens. As shown in Fig. 2F, in HCC samples, the expression levels of LCMT1 are positively associated with the expression levels of GLUT1, HK2, PKF2, PKM, LDHA, and MCT4. These results strongly support the results shown above. All these results indicate that LCMT1 drives the metabolic reprogramming of glycolysis in HCC cells.

Silencing LCMT1 promoted mitochondrial dysfunction

Some studies have reported that the suppression of glycolysis in cancer cells may restore mitochondrial oxidative phosphorylation (OXPHOS). The restoration of OXPHOS can be a hot spot for tumor therapy [26]. Therefore, it is interesting to know whether the inhibition
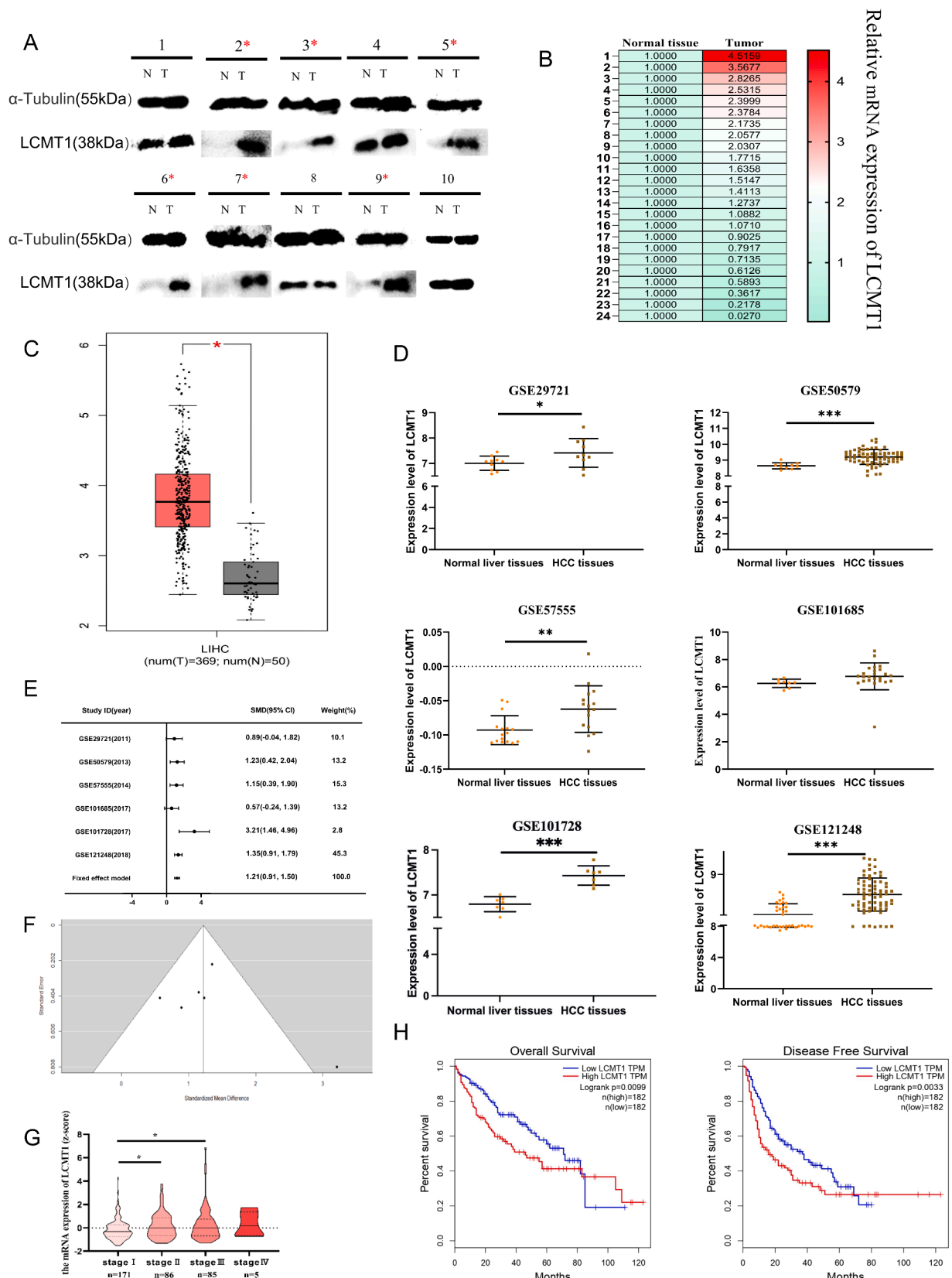
Fig. 1. LCMT1 was upregulated in HCC patients and was a poor prognostic factor. (A) The protein expression levels of LCMT1 in HCC tissues and adjacent non-tumorous liver tissues. (B) The mRNA expression levels of LCMT1 in HCC tissues and adjacent nontumorous liver tissues. (C) The RNA-seq data on the expression levels of LCMT1 in 50 nontumorous liver specimens and 369 HCC patients. (D) The expression levels of LCMT1 in nontumorous tissues and HCC tissues. The data were obtained from GEO datasets. (E-F) A meta-analysis was carried out under the fixed-effect model, and an analysis of publication bias was performed. (G) In HCC patients, the expression levels of LCMT1 were associated with the stages of the tumor. (H) The mRNA expression level of LCMT1 correlated with the OS and DFS of HCC patients.

Table 1

Basic information and LCMT1 expression levels in Gene expression omnibus (GEO) datasets.

GEO datesets	Year	Platform	Country	Tissues type	N	LCMT1 expression (X±SD)	t	P
GSE29721	2011	GPL570	Canada	Normal tissue	10	7.00±0.27	-2.12	0.045
				HCC tissue	10	7.41±0.56		
GSE50579	2013	GPL14550	Germany	Normal tissue	7	8.92±0.10	3.52	<0.001
				HCC tissue	60	9.19±0.46		
GSE57555	2014	GPL16699	Japan	Normal tissue	16	-0.09±0.02	-3.08	0.004
				HCC tissue	16	-0.06±0.03		
GSE101685	2017	GPL570	China Taiwan	Normal tissue	8	6.26±0.3	-1.49	0.146
				HCC tissue	24	6.77±0.98		
GSE101728	2017	GPL21047	China	Normal tissue	7	6.79±0.16	5.69	<0.001
				HCC tissue	7	7.43±0.21		
GSE121248	2018	GPL570	Singapore	Normal tissue	37	8.11±0.24	6.68	<0.001
				HCC tissue	70	8.55±0.36		

Table 2

Relationship between LCMT1 expression level and clinical characteristics features in TCGA data set.

Clinical characteristics		N	Expression level of LCMT1 Low	High	χ^2	p
Diagnosis Age	<50	77	32	45	2.868	0.09
	≥50	290	152	138		
Gender	Male	249	124	125	0.035	0.852
	Female	120	61	59		
Race	Asian	158	67	91	6.981	0.008
	Non-Asian	202	114	88		
Alcohol Consumption	YES	118	53	65	2.39	0.112
	NO	233	125	108		
HBV Infection	YES	103	53	50	0.014	0.907
	NO	184	96	88		
Histologic Grade	1-2	230	127	103	7.538	0.006
	3-4	134	54	80		
Tumor Size	≤3cm	181	102	79	6.254	0.012
	>3cm	187	81	106		
Vascular Invasion	None	206	111	95	3.304	0.069
	Micro/Macro	109	47	62		
Family History	YES	111	67	44	6.639	0.01
	NO	258	118	140		

on glycolysis restores OXPHOS in LCMT1-silenced HCC cells. We detected the changes in mitochondrial function in LCMT1-silenced HepG2 cells and LCMT1-silenced Huh7 cells. The mitochondrial content was examined by MitoTracker Green. After LCMT1 silencing, the fluorescence intensity of Mito-Tracker Green decreased (Fig. 3A), which indicates that LCMT1 silencing results in low mitochondrial mass. MMP was analyzed by JC-1 staining. In LCMT1-silenced cells, J-aggregates changed into their monomers, and the emitted fluorescence switched from red to green (Fig. 3B), which indicates that MMP declines markedly in LCMT1-silenced cells, and the cells are in a mitochondrial-dysfunction state. Mitochondria produce ATP through the tricarboxylic acid (TCA) cycle. This cycle is initiated by the oxidation of pyruvate to acetyl CoA. The acetyl CoA is oxidized to produce ATP. In response to the oxidation of acetyl CoA, mitochondrial pyruvate carrier 1 (MPC1), which is a specific carrier in the inner mitochondrial membrane, imports pyruvate from cytoplasm into the mitochondrial matrix, where pyruvate can be oxidized to fuel the TCA cycle and ATP production [27,28]. We detected that the expression of MPC1 in LCMT1-silenced cells reduced significantly (Fig. 3C). Mitochondria also produce ROS, which are intrinsic by-products of ATP production. Cancer cells are characterized by ROS overproduction, which promotes cancer development [29,30]. We quantified intracellular ROS levels by DCFH-DA and found that the ROS levels in LCMT1-silenced cells were significantly lower than the ROS levels in control cells (Fig. 3D). RSS is a redox-sensitive dye that can be reduced to resorufin by the mitochondrial respiratory chain. RSS acts as an intermediate electron acceptor in the electron transport chain. As shown in Fig. 3E, in LCMT1-silenced cells, the fluorescence intensity of

RSS decreases significantly, which suggests that the mitochondrial redox capacity of the cells reduces. All these results indicate that LCMT1 silencing promotes mitochondrial dysfunction, and OXPHOS is not restored in LCMT1-silenced cells, in which glycolysis is inhibited.

LCMT1 silencing upregulated the expression of AGXT and promoted the biosynthesis of pyruvate

Pyruvate, which is produced by glycolysis, is a raw material for aerobic and anaerobic respiration of cells. The metabolism of pyruvate is altered during cancer progression [31,32]. We detected the intracellular pyruvate level and found that silencing LCMT1 increased the intracellular pyruvate level (Fig. 4A). Since glycolysis and OXPHOS were downregulated in LCMT1-silenced HCC cells, from a point of view of energy metabolism, it is hard to explain why the intracellular pyruvate level increased. However, pyruvate is produced in protein metabolism, which produces amino acids, and in carbohydrate metabolism, which produces monosaccharides. Some amino acids, such as alanine, glycine and serine can be converted to pyruvate by transamination. Therefore, we analyzed whether amino acid metabolism contributes to the increase in the intracellular pyruvate level. We quantified the levels of free amino acids in the culture medium of LCMT1-silenced cells. Twenty-two amino acids were detected, and the levels of alanine, glycine and serine were observed to increase significantly (Fig. 4B). Using search tool for interactions of chemicals (STITCH), we constructed a gene–metabolite interaction network. The database integrates information about interactions from metabolic pathways, crystal structures, binding experiments, and drug–target relationships [33–35]. The AGXT node was the node with the highest degree and the highest betweenness (Fig. 4C). Then, we used the gene module of (National Center for Biotechnology Information) NCBI to explore the pathways related to AGXT. The "pyruvate biosynthetic process" was enriched. In addition, in the TCGA dataset, LCMT1 was negatively associated with AGXT (Fig. 4D). Further, we detected that AGXT was upregulated in LCMT1-silenced cells (Fig. 4E). To confirm whether LCMT1 increased the intracellular pyruvate level by upregulating the expression of AGXT, in HepG2 and Huh7 cells, we silenced both AGXT and LCMT1. We found that silencing both AGXT and LCMT1 reduced the intracellular pyruvate level, which increased after LCMT1 silencing (Fig. 4F). The result indicates that LCMT1 silencing increases the intracellular pyruvate level by upregulating the expression of AGXT.

LCMT1 promoted the proliferation of HCC cells

Changes to pyruvate metabolism play an important regulatory role in the development of cancer [36]. It has been reported that pyruvate supplementation can affect the proliferation of tumor cells [37]. Therefore, we analyzed whether the increase in the intracellular pyruvate level affects the proliferation of HCC. The CCK-8 assay and EdU assay were used to determine the proliferation of LCMT1-silenced and LCMT1-overexpressed cells. In LCMT1-silenced cells, the number of
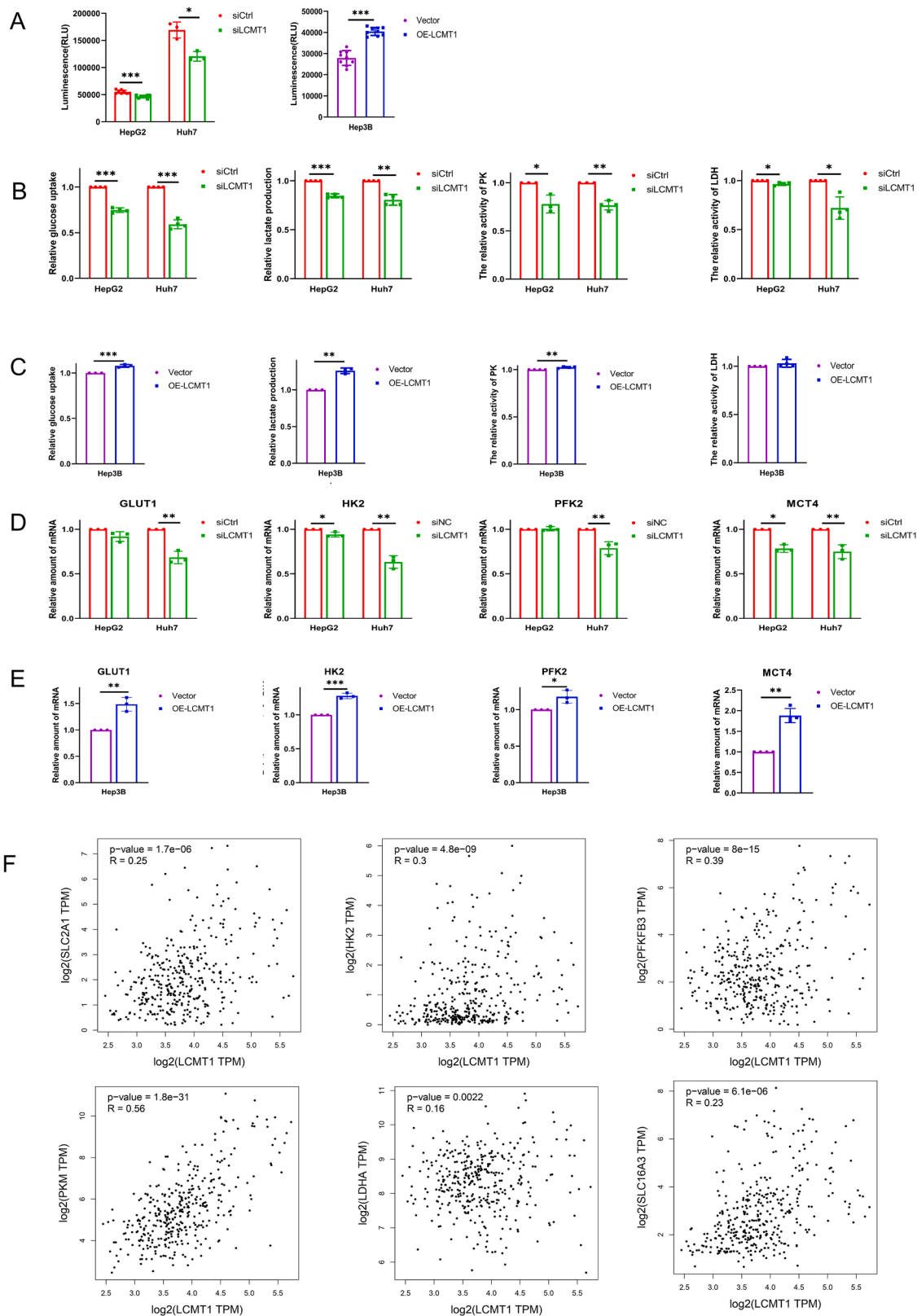
Fig. 2. LCMT1 drove metabolic reprogramming of glycolysis in HCC cells. (A) The levels of ATP in LCMT1 silenced HepG2 and Huh7 cells, or overexpressed Hep3B cell. (B) The uptake of glucose, production of lactate, activity of PK, and activity of LDH in HepG2 and Huh7 cells in which LCMT1 was silenced. (C) The uptake of glucose, production of lactate, activity of PK, and activity of LDH in Hep3B cells in which LCMT1 was overexpressed. (D) The expression levels of the mRNA for GLUT1, mRNA for HK2, mRNA for PFK2, and mRNA for MCT4 in HepG2 and Huh7 cells in which LCMT1 was silenced. The mRNA expression levels were determined by RT-PCR. (E) The expression levels of the mRNA for GLUT1, mRNA for HK2, mRNA for PFK2, and mRNA for MCT4 in Hep3B cells in which LCMT1 was over-expressed. The mRNA expression levels were determined by RT-PCR. (F) The relationships between LCMT1 and the key glycolytic genes. The regression analyses were performed by GEPIA.
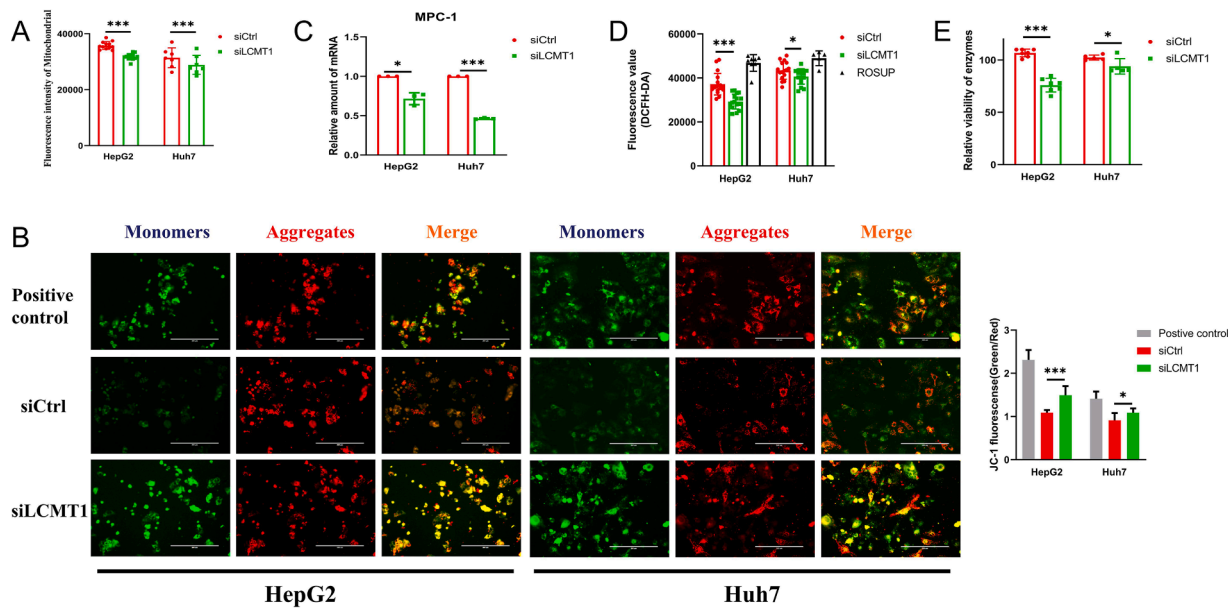
Fig. 3. Silencing LCMT1 promoted mitochondrial dysfunction. (A) The intensities of the fluorescence emitted by LCMT1-silenced HepG2 cells and LCMT1-silenced Huh7 cells. The fluorescence intensities were examined by MitoTracker Green and were detected by a Multiskan Spectrum spectrophotometer. (B) Observations of the stained mitochondria by an inverted fluorescence microscope. The determination of the intensities of the fluorescence emitted by LCMT1-silenced HepG2 cells and LCMT1-silenced Huh7 cells by a Multiskan Spectrum spectrophotometer. (C) The mRNA expression levels of MPC-1 in HepG2 and Huh7 cells in which LCMT1 was silenced. The mRNA expression levels were determined by RT-PCR. (D) The fluorescence intensities of DCFH-DA in HepG2 and Huh7 cells in which LCMT1 was silenced. The fluorescence intensities were detected by a Multiskan Spectrum spectrophotometer. (E) The fluorescence intensities of cyclophorase-reacted RSS in HepG2 and Huh7 cells in which LCMT1 was silenced. The fluorescence intensities were detected by a Multiskan Spectrum spectrophotometer.
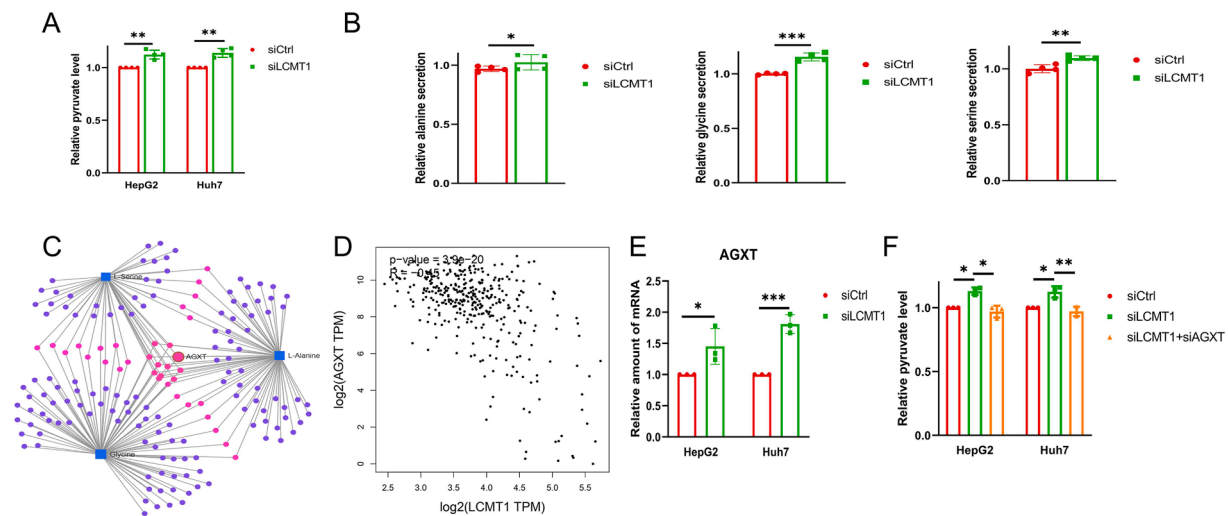
Fig. 4. LCMT1 silencing upregulated the expression of AGXT and promoted the biosynthesis of pyruvate. (A) The effects of LCMT1 on the intracellular levels of pyruvate in HepG2 and Huh7 cells. (B) The effects of LCMT1 on the levels of alanine, glycine, and serine in HepG2 cells. The levels of the amino acids were determined by the HPLC–UV method. (C) A gene–metabolite network showing interactions between LCMT1 and the amino acids. The gene–metabolite network analysis was performed by STITCH. (D) The relationship between LCMT1 and AGXT. The regression analysis was performed by GEPIA. (E) The RT-PCR determination of the mRNA expression of AGXT in HepG2 and Huh7 cells in which LCMT1 was silenced. (F) The effects of silencing LCMT1 and AGXT on the intracellular levels of pyruvate in HepG2 and Huh7cells.

S-phase cells, which was indicated by the EdU assay, diminished significantly

(Fig. 5A), and the proliferation of the LCMT1-silenced cells, which was indicated by the CCK-8 assay, weakened distinctly (Fig. 5B). MKI67, which is a nucleoprotein expressed in all phases of the cell cycle except the G_0 phase, was significantly downregulated in LCMT1-silenced HepG2 cells (Fig. 5C). Compared to the expression of MK167 in Hep3B cells transfected with the blank vector, the expression of MKI67 in LCMT1-overexpressed Hep3B cells increased (Fig. 5D). The CCK-8

assay and the EdU assay showed opposite results (Fig. 5E and F), which indicates that the overexpression of LCMT1 promotes cell proliferation. Furthermore, gene ontology (GO) enrichment analysis showed that the GO terms related to cell growth and proliferation, such as "spindle checkpoint", "positive regulation of microtubule depolymerization", and "regulation of cell growth", were significantly enriched (Fig. 5G), which further supports the experimental results shown above. To confirm whether the upregulation of AGXT, which was induced by LCMT1 silencing, inhibits cell proliferation, we examined the
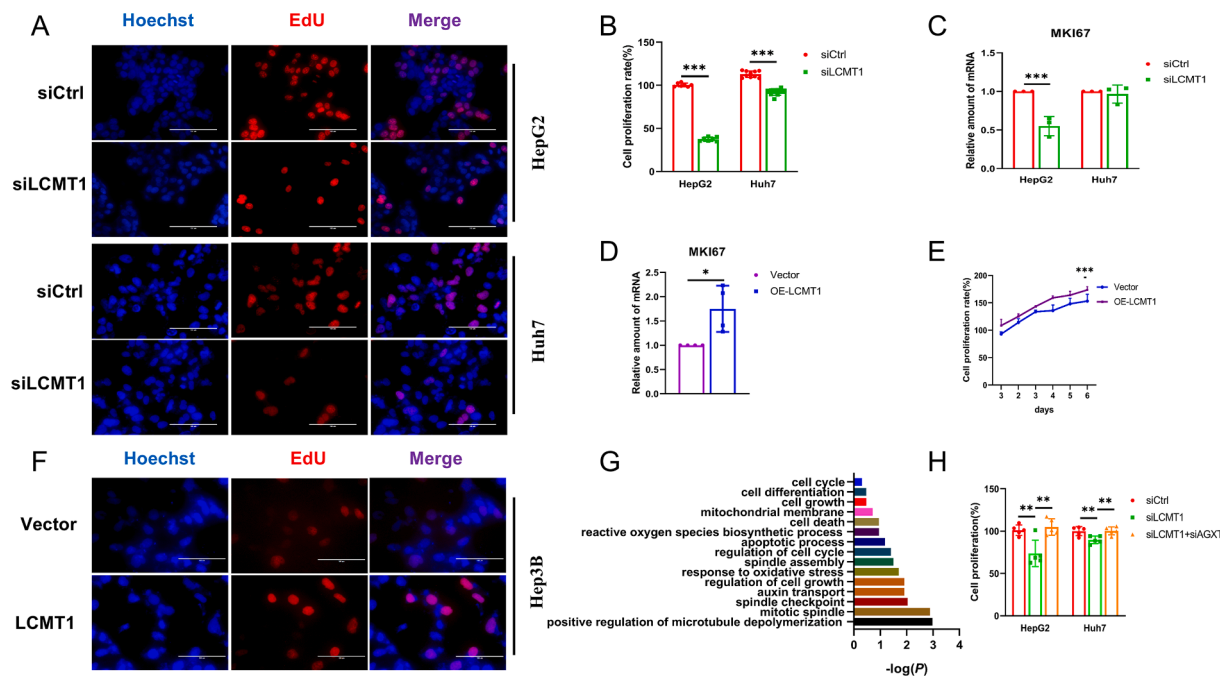
Fig. 5. LCMT1 promoted the proliferation of HCC cells. (A and B) The effects of LCMT1 on the proliferation of HepG2 and Huh7 cells. The proliferation of the cells is determined by (A) the EdU assay and (B) the CCK8 assay. (C) The RT-PCR determination of the mRNA expression of MKI67 in HepG2 and Huh7 cells in which LCMT1 was silenced. (D) The RT-PCR determination of the mRNA expression of MKI67 in Hep3B cells in which LCMT1 was overexpressed. (E and F) The effect of LCMT1 on the proliferation of Hep3B cells. The proliferation of the cells was determined by (E) the CCK8 assay and (F) the EdU assay. (G) The enriched GO terms revealed by the gene enrichment analysis of LCMT1. (H) The effects of silencing LCMT1 and AGXT on the proliferation of HepG2 and Huh7 cells. The proliferation of the cells was determined by the CCK8 assay.

proliferation of cells in which both AGXT and LCMT1 were silenced. Silencing AGXT reversed the inhibitory effect of LCMT1 silencing on cell proliferation almost completely (Fig. 5H), which indicates that LCMT1 silencing suppresses HCC proliferation by upregulating AGXT expression.

Downregulation of LCMT1 expression inhibited the growth of the tumor in the mouse subcutaneous tumor model

To confirm the impact of LCMT1 on HCC *in vivo*, we examined whether an intratumoral injection of siLCMT1 affects tumor growth in a subcutaneous Huh7 xenograft model. After four weeks of Huh7 inoculation, measurable tumor growth was achieved in > 98% of nude mice. After the injection of siLCMT1, tumor growth was remarkably suppressed. The changes in the volume of the tumor after siRNA delivery are shown in Fig. 6A. Compared to the size of the tumors in mice injected with control siRNA, the size of the tumors in mice treated with siLCMT1 declined by about 50% (Fig. 6B). H&E staining analysis showed that tumors treated with siLCMT1 had markedly less necrosis compared to tumors treated with siCtrl (Fig. 6C). Moreover, the treatment with
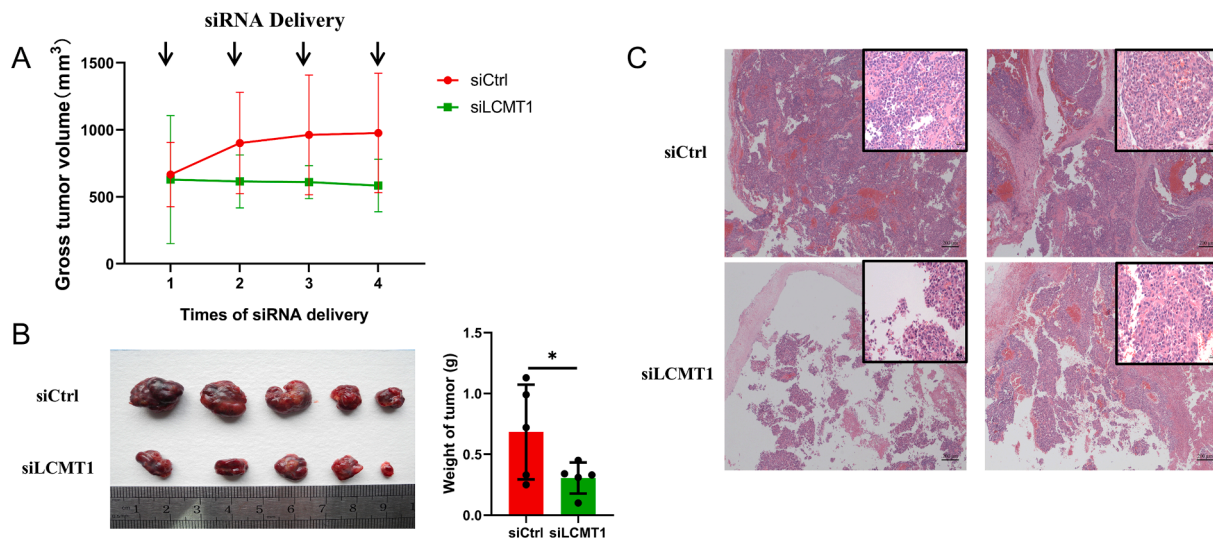
Fig. 6. The downregulation of LCMT1 inhibited the growth of the tumor in the mouse subcutaneous tumor model. (A and B) The growth of the tumor was represented by the volume and weight of the tumor, which were measured for the duration of the experiment. (C) Representative images of the tumor after H&E staining.

siLCMT1 reduced the number of stained tumor cells.

Regulation of HCC proliferation by LCMT1 was related to PP2A

LCMT1 is the only methylase known to catalyze the transfer of methyl groups from SAM to PP2Ac. Fig. 7A shows that LCMT1 silencing increases the expression level of demethylated-PP2Ac (dem-PP2Ac), but it has no significant effect on the expression levels of total PP2Ac and its phosphatase methylesterase (PME). To further explore whether LCMT1 regulates HCC proliferation by regulating the function of PP2A, we used a PP2A inhibitor and a PP2A activator to determine the impact of PP2A inhibition or activation on the proliferation of LCMT1-silenced cells or LCMT-overexpressed HCC cells. Forskolin (FSK), which is a PP2A agonist, was used in LCMT1-silenced Huh7 and HepG2 cells. Okadaic acid (OA), which is an inhibitor of PP2A, was used in LCMT1-overexpressed Hep3B cells. OA treatment alone inhibited the proliferation of HCC, and FSK treatment alone promoted the proliferation of HCC (Fig. 7B andC). In LCMT1-silenced cells, FSK reversed the inhibited cell proliferation induced by LCMT1 silencing (Fig. 7D). As expected, OA decreased the high proliferation of LCMT1-overexpressed cells (Fig. 7E). These results indicate that LCMT1 regulates the proliferation of HCC cells by regulating the function of PP2A.

Discussion

Pyruvate is an important metabolic intermediate. It is key to the intersection between glycolysis and oxidative phosphorylation and is important to the homeostasis of carbohydrates, fats, and amino acids [36]. Metabolic plasticity allows cancer cells to adapt their pyruvate metabolism. Pyruvate, which has antioxidant properties [38], is a precursor for the biosynthesis of glutathione. Therefore, tumor cells maintain a certain level of pyruvate to sustain their growth during hypoxia. It has been reported that pyruvate promotes the production of hypoxia-inducible factor 1 (HIF-1) to support the survival of cancer cells [37]. However, high levels of pyruvate have been reported to suppress the expression of histone genes and inhibit the proliferation of tumor cells [37]. In LCMT1-silenced HepG2 cells and LCMT1-silenced Huh7 cells, the metabolism (production and consumption) of pyruvate was altered. The cellular production of pyruvate through glycolysis was reduced, which was indicated by the downregulation of GLUT1, HK2, PFK2, and MCT4. In the tumor cells, the dominant consumption of pyruvate was diverted to lactate fermentation mediated by LDHA. The lactate fermentation was inhibited, and the TCA cycle was suppressed, which was indicated by the downregulation of MPC-1. The inhibition on glycolysis and the inhibition on the TCA cycle decreased the production of ATP after LCMT1 silencing. However, we detected an increase in the pyruvate biosynthetic process, which was mediated by the upregulation of AGXT expression. Silencing both LCMT1 and AGXT reversed the
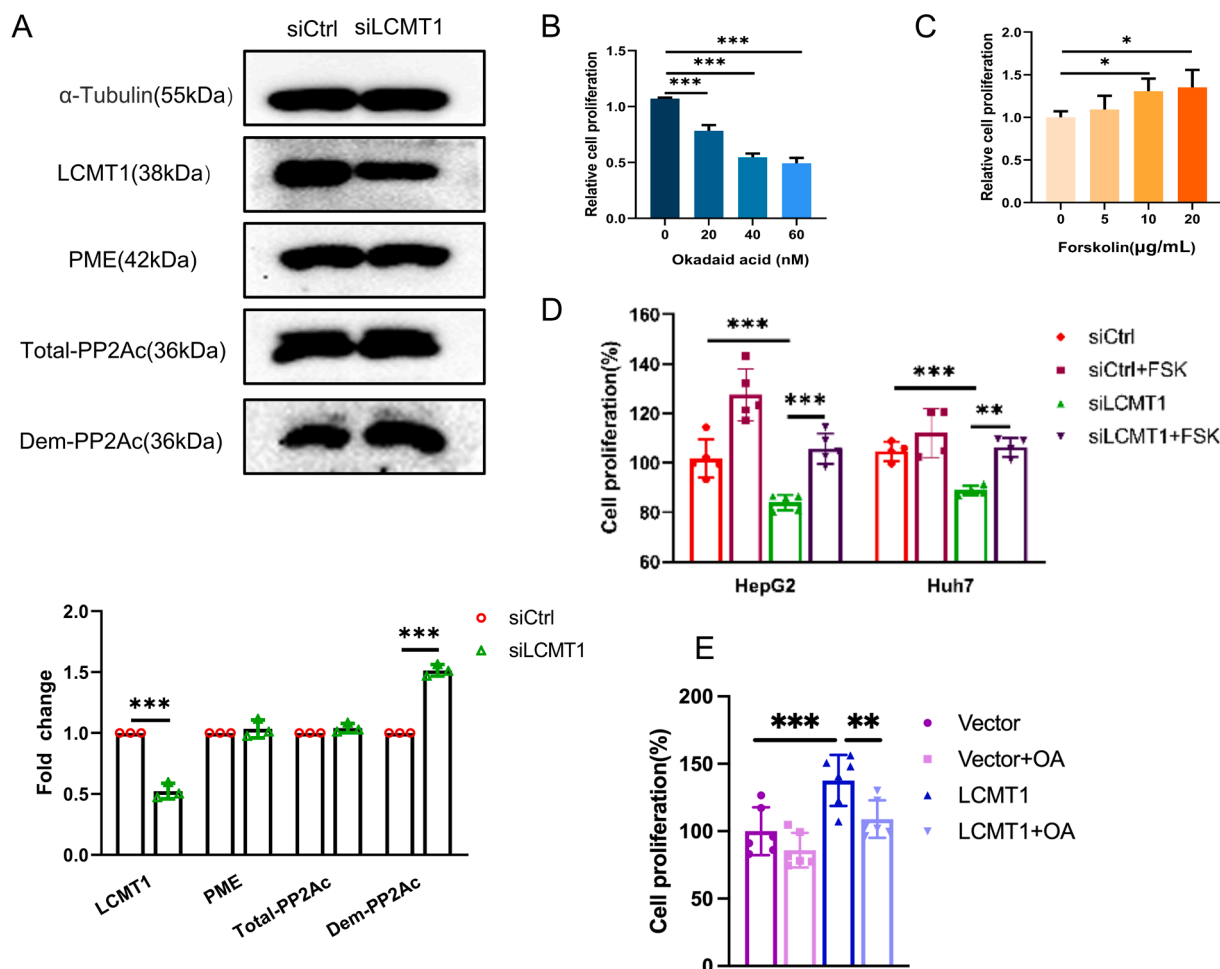
Fig. 7. The regulation of HCC proliferation by LCMT1 was partly related to PP2Ac. (A) A western blotting analysis of the levels of LCMT1, PME, total PP2Ac, and Dem-PP2Ac in HepG2 cells in which LCMT1 was silenced. (B) The effect of OA on Hep3B cells and (C) the effect of FSK on Huh7 cells. (D) The effects of FSK on the proliferation of HepG2 and Huh7 cells in which LCMT1 was silenced. The proliferation of the cells was determined by the CCK8 assay. (E) The effect of OA on the proliferation of Hep3B cells in which LCMT1 was overexpressed. The proliferation of the cells was determined by the CCK8 assay.

increase in the intracellular pyruvate level and the decrease in HCC proliferation, which suggests that LCMT1 silencing increases the intracellular pyruvate level and inhibits HCC proliferation by upregulating the expression of AGXT.

The *AGXT* gene is expressed mainly in the liver, and its encoded protein is localized mostly in peroxisomes. The mutation or dysfunction of the *AGXT* gene contributes to the accumulation of glyoxylate, which results in the overproduction of oxalate and development of primary hyperoxaluria type I [39]. In the peroxisomal matrix, AGXT catalyzes the transamination of L-alanine to pyruvate and transamination of glyoxylate to glycine. It is an enzyme dependent on pyridoxal 5′-phosphate (PLP). In the first step, in its PLP form (AGXT–PLP), the enzyme reacts with L-alanine and generates pyruvate and the pyridoxamine 5′-phosphate form of the enzyme (AGXT–PMP). Then, AGXT–PMP binds to glyoxylate and converts it to glycine and regenerates AGXT–PLP. Since the binding affinity of AGXT for PMP is greatly higher than that of AGXT for PLP, the rate of the catalytic transamination of glyoxylate to glycine is higher than that of the catalytic transamination of L-alanine to pyruvate. Therefore, the primary role of AGXT is the glyoxylate-to-glycine conversion [40]. For that reason, most AGXT studies have focused on glyoxylate detoxification instead of pyruvate biosynthesis. The relationships between AGXT and tumors were initially found through screenings for differential gene expression in tumorous and normal tissues. The *AGXT* gene was identified as a hub gene in studies on clear cell renal cell carcinoma [41] and HCC [42]. Afterwards, correlations between poor prognoses and low expression levels of AGXT in tumors were found. Moreover, AGXT was proposed as a novel marker for HCC, and the potential role of AGXT in tumorigenesis was indicated [42,43]. However, the role of AGXT in the proliferation of tumor cells is unknown. Our results showed that the expression of AGXT regulated the cellular metabolism of pyruvate, which plays a vital role in the proliferation of tumor cells. However, no published documents have reported a direct relationship between LCMT1 and AGXT. Nonetheless, there have been reports on the crosstalk between liver kinase B1 (LKB1), which is a dual (serine/threonine and tyrosine) protein kinase, and PP2A [44,45] to phosphorylate/dephosphorylate adenosine 5′-monophosphate (AMP)-activated protein kinase (AMPK) and to regulate energy balance. Recently, AGXT has been found to be the substrate of LKB1 to regulate amino-acid-driven gluconeogenesis in the liver [46]. Therefore, LCMT1 may regulate the expression of AGXT by regulating the PP2A/LKB1 signaling pathway. Further studies are needed to prove this hypothesis.

Even though LCMT1 methylates the terminal carboxyl groups of the leucine-309 residues of PP2A, PP4, and PP6, undisputedly, PP2A is the most studied substrate of LCMT1. PP2A is generally accepted as a tumor suppressor that reverses the phosphorylation of oncoproteins [47]. However, the *PPP2CA* gene has shown similar characteristics to a proto-oncogene [48]. The results obtained from HCC patients are consistent with the results reported in our previous paper [49] and several other papers [50,51]. The expression of PP2A in HCC tissue was significantly higher than that of PP2A in nontumorous liver tissue. The HCC tissue and nontumorous liver tissue were obtained from the same patients. Multivariate analysis revealed that the upregulation of PP2A predicts a poor prognosis and is associated with shorter overall survival, shorter progression-free survival, and shorter disease-free survival [49, 51]. *In vitro* and *in vivo*, the inhibition of PP2A enhances the cytotoxicity of chemotherapy to HCC [52] and restricts the growth and metastasis of HCC [53]. The evidence supports the hypothesis that the *PPP2CA* gene acts like an oncogene in HCC patients. Therefore, in HCC patients, regulating the function of PP2A, the LCMT1 gene may act as an oncogene necessary to the proliferation of HCC cells.

Our study has several limitations. Firstly, we only explored the data in public datasets to demonstrate that a high level of LCMT1 predicted a poor prognosis and to detect the expression levels of LCMT1 in a small group of patients from a single geographical region. Therefore, the results need to be validated by using large high-quality prospective

cohorts. Secondly, we did not detect how LCMT1 regulated the expression of AGXT. Thirdly, the potential impact of LCMT1 on glycolytic genes should be confirmed by western blotting.

In summary, our results showed that LCMT1 silencing drove the metabolic reprogramming of glycolysis and induced the cellular accumulation of pyruvate to inhibit the proliferation of HCC cells. The results indicate that LCMT1 may be a novel biomarker for HCC and a potential target for tumor therapy.

Ethical approval

All study procedures were performed on approval by the Ethics Committee of Guangxi Medical University and the Animal Care & Welfare Committee of Guangxi Medical University.The approval code is 20210144.

Funding

Supplementary Fig. The validation of the transfection of siRNA and overexpression of LCMT1 in (A and D) HepG2 cells, (B and E) Huh7 cells, and (C and F) Hep3B cells. Fluorescence spectroscopy and western blotting were applied to the validation.

CRediT authorship contribution statement

Ning Zhang: Conceptualization, Methodology, Investigation, Writing – original draft, Writing – review & editing. **Cailing Lu:** Conceptualization, Writing – review & editing, Funding acquisition. **Jiao Mo:** Investigation, Writing – original draft. **Xinhang Wang:** Methodology, Writing – original draft. **Simi Liao:** Investigation. **Ningjing Liang:** Investigation. **Mei Feng:** Investigation. **Tingting Tang:** Investigation. **Yijie Wu:** Investigation. **Yunqing Li:** Investigation. **Chunhua Lan:** Investigation. **Chengying Chen:** Investigation. **Qianqian Shi:** Investigation. **Lancheng Wei:** Investigation. **Zhijian Zheng:** . **Yu Lei:** . **Zhiming Zhang:** Resources. **Shen Tang:** Methodology, Writing – review & editing, Funding acquisition, Resources. **Xiyi Li:** Conceptualization, Methodology, Writing – review & editing, Funding acquisition, Supervision.

Declaration of Competing Interest

All authors declare no conflict of interests.

Supplementary materials

Supplementary material associated with this article can be found, in the online version, at doi:10.1016/j.tranon.2022.101572.

References

[1] e.e.e. European Association for the Study of the Liver, Electronic address, L. European Association for the study of the, EASL clinical practice guidelines: management of hepatocellular carcinoma, J. Hepatol. 69 (2018) 182–236, https://doi.org/10.1016/j.jhep.2018.03.019.

[2] H. Sung, J. Ferlay, R.L. Siegel, M. Laversanne, I. Soerjomataram, A. Jemal, F. Bray, Global cancer statistics 2020: GLOBOCAN estimates of incidence and mortality worldwide for 36 cancers in 185 countries, CA Cancer J. Clin. 71 (2021) 209–249, https://doi.org/10.3322/caac.21660.

[3] A. Forner, M. Reig, J. Bruix, Hepatocellular carcinoma, Lancet 391 (2018) 1301–1314, https://doi.org/10.1016/S0140-6736(18)30010-2.

[4] K.S. Rallis, D. Makrakis, I.A. Ziogas, G. Tsoulfas, Immunotherapy for advanced hepatocellular carcinoma: From clinical trials to real-world data and future advances, %J, World J. Clin. Oncol. 13 (2022) 448–472.

[5] S. De Lorenzo, F. Tovoli, M.A. Barbera, F. Garuti, A. Palloni, G. Frega, I. Garajova, A. Rizzo, F. Trevisani, G. Brandi, Metronomic capecitabine vs. best supportive care

in Child-Pugh B hepatocellular carcinoma: a proof of concept, Sci. Rep. 8 (2018) 9997, https://doi.org/10.1038/s41598-018-28337-6.

[6] A. Rizzo, A.D. Ricci, PD-L1, TMB, and other potential predictors of response to immunotherapy for hepatocellular carcinoma: how can they assist drug clinical trials? Expert Opin. Investig. Drugs 31 (2022) 415–423, https://doi.org/10.1080/13543784.2021.1972969.

[7] A. Rizzo, A.D. Ricci, G. Gadaleta-Caldarola, G. Brandi, First-line immune checkpoint inhibitor-based combinations in unresectable hepatocellular carcinoma: current management and future challenges, Expert Rev. Gastroenterol. Hepatol. 15 (2021) 1245–1251, https://doi.org/10.1080/17474124.2021.1973431.

[8] L. Fagerberg, B.M. Hallstrom, P. Oksvold, C. Kampf, D. Djureinovic, J. Odeberg, M. Habuka, S. Tahmasebpoor, A. Danielsson, K. Edlund, A. Asplund, E. Sjostedt, E. Lundberg, C.A. Szigyarto, M. Skogs, J.O. Takanen, H. Berling, H. Tegel, J. Mulder, P. Nilsson, J.M. Schwenk, C. Lindskog, F. Danielsson, A. Mardinoglu, A. Sivertsson, K. von Feilitzen, M. Forsberg, M. Zwahlen, I. Olsson, S. Navani, M. Huss, J. Nielsen, F. Ponten, M. Uhlen, Analysis of the human tissue-specific expression by genome-wide integration of transcriptomics and antibody-based proteomics, Mol. Cell. Proteomics 13 (2014) 397–406, https://doi.org/10.1074/mcp.M113.035600.

[9] Y. Xing, Z. Li, Y. Chen, J.B. Stock, P.D. Jeffrey, Y. Shi, Structural mechanism of demethylation and inactivation of protein phosphatase 2A, Cell 133 (2008) 154–163, https://doi.org/10.1016/j.cell.2008.02.041.

[10] J. Hwang, J.A. Lee, D.C. Pallas, Leucine carboxyl methyltransferase 1 (LCMT-1) methylates protein phosphatase 4 (PP4) and protein phosphatase 6 (PP6) and differentially regulates the stable formation of different PP4 holoenzymes, J. Biol. Chem. 291 (2016) 21008–21019, https://doi.org/10.1074/jbc.M116.739920.

[11] R.E. Nicholls, J.M. Sontag, H. Zhang, A. Staniszewski, S. Yan, C.Y. Kim, M. Yim, C. M. Woodruff, E. Arning, B. Wasek, D. Yin, T. Bottiglieri, E. Sontag, E.R. Kandel, O. Arancio, PP2A methylation controls sensitivity and resistance to beta-amyloid-induced cognitive and electrophysiological impairments, Proc. Natl. Acad. Sci. USA. 113 (2016) 3347–3352, https://doi.org/10.1073/pnas.1521018113.

[12] H.J. Park, K.W. Lee, E.S. Park, S. Oh, R. Yan, J. Zhang, T.G. Beach, C.H. Adler, M. Voronkov, S.P. Braithwaite, J.B. Stock, M.M. Mouradian, Dysregulation of protein phosphatase 2A in Parkinson disease and dementia with Lewy bodies, Ann. Clin. Transl. Neurol. 3 (2016) 769–780, https://doi.org/10.1002/acn3.337.

[13] Y. Xu, L. Wei, S. Tang, Q. Shi, B. Wu, X. Yang, Y. Zou, X. Wang, Q. Ao, L. Meng, X. Wei, N. Zhang, Y. Li, C. Lan, M. Chen, X. Li, C. Lu, Regulation PP2Ac methylation ameliorating autophagy dysfunction caused by Mn is associated with mTORC1/ULK1 pathway, Food Chem. Toxicol. 156 (2021) 112441, https://doi.org/10.1016/j.fct.2021.112441.

[14] B. Wu, H. Cai, S. Tang, Y. Xu, Q. Shi, L. Wei, L. Meng, N. Zhang, X. Wang, D. Xiao, Y. Zou, X. Yang, X. Li, C. Lu, Methionine-mediated protein phosphatase 2A catalytic subunit (PP2Ac) methylation ameliorates the tauopathy induced by manganese in cell and animal models, Neurotherapeutics 17 (2020) 1878–1896, https://doi.org/10.1007/s13311-020-00930-6.

[15] J.M. Sontag, V. Nunbhakdi-Craig, L. Montgomery, E. Arning, T. Bottiglieri, E. Sontag, Folate deficiency induces *in vitro* and mouse brain region-specific downregulation of leucine carboxyl methyltransferase-1 and protein phosphatase 2A B(alpha) subunit expression that correlate with enhanced tau phosphorylation, J. Neurosci. 28 (2008) 11477–11487, https://doi.org/10.1523/JNEUROSCI.2816-08.2008.

[16] M. Gnanaprakash, A. Staniszewski, H. Zhang, R. Pitstick, M.P. Kavanaugh, O. Arancio, R.E. Nicholls, Leucine carboxyl methyltransferase 1 overexpression protects against cognitive and electrophysiological impairments in Tg2576 APP transgenic mice, J. Alzheimers Dis. 79 (2021) 1813–1829, https://doi.org/10.3233/JAD-200462.

[17] S. Longin, K. Zwaenepoel, J.V. Louis, S. Dilworth, J. Goris, V. Janssens, Selection of protein phosphatase 2A regulatory subunits is mediated by the C terminus of the catalytic Subunit, J. Biol. Chem. 282 (2007) 26971–26980, https://doi.org/10.1074/jbc.M704059200.

[18] M. Brechmann, T. Mock, D. Nickles, M. Kiessling, N. Weit, R. Breuer, W. Muller, G. Wabnitz, F. Frey, J.P. Nicolay, N. Booken, Y. Samstag, C.D. Klemke, M. Herling, M. Boutros, P.H. Krammer, R. Arnold, A PP4 holoenzyme balances physiological and oncogenic nuclear factor-kappa B signaling in T lymphocytes, Immunity 37 (2012) 697–708, https://doi.org/10.1016/j.immuni.2012.07.014.

[19] J.B. Jackson, D.C. Pallas, Circumventing cellular control of PP2A by methylation promotes transformation in an Akt-dependent manner, Neoplasia 14 (2012) 585–599, https://doi.org/10.1593/neo.12768.

[20] K. Schmeisser, J.A. Parker, Nicotinamide-N-methyltransferase controls behavior, neurodegeneration and lifespan by regulating neuronal autophagy, PLos Genet. 14 (2018), e1007561, https://doi.org/10.1371/journal.pgen.1007561.

[21] J.A. Lee, D.C. Pallas, Leucine carboxyl methyltransferase-1 is necessary for normal progression through mitosis in mammalian cells, J. Biol. Chem. 282 (2007) 30974–30984, https://doi.org/10.1074/jbc.M704861200.

[22] S. Tang, F. Qin, X. Wang, Z. Liang, H. Cai, L. Mo, Y. Huang, B. Liang, X. Wei, Q. Ao, Y. Xu, Y. Liu, D. Xiao, S. Guo, C. Lu, X. Li, H₂O₂ induces PP2A demethylation to downregulate mTORC1 signaling in HEK293 cells, Cell Biol. Int. 42 (2018) 1182–1191, https://doi.org/10.1002/cbin.10987.

[23] S.N. Rampersad, Multiple applications of Alamar Blue as an indicator of metabolic function and cellular health in cell viability bioassays, Sensors 12 (2012) 12347–12360, https://doi.org/10.3390/s120912347 (Basel).

[24] L. Li, L. Li, W. Li, T. Chen, Z. Bin, L. Zhao, H. Wang, X. Wang, L. Xu, X. Liu, D. Wang, B. Li, T.W. Mak, W. Du, X. Yang, P. Jiang, TAp73-induced phosphofructokinase-1 transcription promotes the Warburg effect and enhances

[25] K. Xu, N. Yin, M. Peng, E.G. Stamatiades, A. Shyu, P. Li, X. Zhang, M.H. Do, Z. Wang, K.J. Capistrano, C. Chou, A.G. Levine, A.Y. Rudensky, M.O. Li, Glycolysis fuels phosphoinositide 3-kinase signaling to bolster T cell immunity, Science 371 (2021) 405–410, https://doi.org/10.1126/science.abb2683.

[26] H. Nie, H. Ju, J. Fan, X. Shi, Y. Cheng, X. Cang, Z. Zheng, X. Duan, W. Yi, O-GlcNAcylation of PGK1 coordinates glycolysis and TCA cycle to promote tumor growth, Nat. Commun. 11 (2020) 36, https://doi.org/10.1038/s41467-019-13601-8.

[27] C. Corbet, E. Bastien, N. Draoui, B. Doix, L. Mignion, B.F. Jordan, A. Marchand, J. C. Vanherck, P. Chaltin, O. Schakman, H.M. Becker, O. Riant, O. Feron, Interruption of lactate uptake by inhibiting mitochondrial pyruvate transport unravels direct antitumor and radiosensitizing effects, Nat. Commun. 9 (2018) 1208, https://doi.org/10.1038/s41467-018-03525-0.

[28] S. Herzig, E. Raemy, S. Montessuit, J.L. Veuthey, N. Zamboni, B. Westermann, E. R. Kunji, J.C. Martinou, Identification and functional expression of the mitochondrial pyruvate carrier, Science 337 (2012) 93–96, https://doi.org/10.1126/science.1218530.

[29] K Ishikawa, K Takenaga, M Akimoto, N Koshikawa, A Yamaguchi, H Imanishi, K Nakada, Y Honma, J Hayashi, ROS-generating mitochondrial DNA mutations can regulate tumor cell metastasis, Science 320 (2008) 661–664, https://doi.org/10.1126/science.1156906.

[30] A.J. Robinson, G.L. Hopkins, N. Rastogi, M. Hodges, M. Doyle, S. Davies, P.S. Hole, N. Omidvar, R.L. Darley, A. Tonks, Reactive oxygen species drive proliferation in acute myeloid leukemia via the glycolytic regulator PFKFB3, Cancer Res. 80 (2020) 937–949, https://doi.org/10.1158/0008-5472.CAN-19-1920.

[31] J. Cui, M. Quan, D. Xie, Y. Gao, S. Guha, M.B. Fallon, J. Chen, K. Xie, A novel KDM5A/MPC-1 signaling pathway promotes pancreatic cancer progression via redirecting mitochondrial pyruvate metabolism, Oncogene 39 (2020) 1140–1151, https://doi.org/10.1038/s41388-019-1051-8.

[32] D.A. Cappel, S. Deja, J.A.G. Duarte, B. Kucejova, M. Inigo, J.A. Fletcher, X. Fu, E. D. Berglund, T. Liu, J.K. Elmquist, S. Hammer, P. Mishra, J.D. Browning, S. C. Burgess, Pyruvate-carboxylase-mediated anaplerosis promotes antioxidant capacity by sustaining TCA cycle and redox metabolism in liver, Cell Metab. 29 (2019) 1291–1305, https://doi.org/10.1016/j.cmet.2019.03.014, e1298.

[33] J. Huang, C. Niu, C.D. Green, L. Yang, H. Mei, J.D. Han, Systematic prediction of pharmacodynamic drug-drug interactions through protein-protein-interaction network, PLoS Comput. Biol. 9 (2013), e1002998, https://doi.org/10.1371/journal.pcbi.1002998.

[34] W. Schaal, U. Hammerling, M.G. Gustafsson, O. Spjuth, Automated QuantMap for rapid quantitative molecular network topology analysis, Bioinformatics 29 (2013) 2369–2370, https://doi.org/10.1093/bioinformatics/btt390.

[35] D. Szklarczyk, A. Santos, C. von Mering, L.J. Jensen, P. Bork, M. Kuhn, STITCH 5: augmenting protein-chemical interaction networks with tissue and affinity data, Nucl. Acids Res. 44 (2016) D380–D384, https://doi.org/10.1093/nar/gkv1277.

[36] G. Bergers, S.M. Fendt, The metabolism of cancer cells during metastasis, Nat. Rev. Cancer 21 (2021) 162–180, https://doi.org/10.1038/s41568-020-00320-2.

[37] R. Ma, Y. Wu, Y. Zhai, B. Hu, W. Ma, W. Yang, Q. Yu, Z. Chen, J.L. Workman, X. Yu, S. Li, Exogenous pyruvate represses histone gene expression and inhibits cancer cell proliferation via the NAMPT-NAD+-SIRT1 pathway, Nucl. Acids Res. 47 (2019) 11132–11150, https://doi.org/10.1093/nar/gkz864.

[38] E. Roudier, C. Bachelet, A. Perrin, Pyruvate reduces DNA damage during hypoxia and after reoxygenation in hepatocellular carcinoma cells, FEBS J. 274 (2007) 5188–5198, https://doi.org/10.1111/j.1742-4658.2007.06044.x.

[39] G. Mandrile, C.S. van Woerden, P. Berchialla, B.B. Beck, C. Acquaviva Bourdain, S. A. Hulton, G. Rumsby, C. OxalEurope, Data from a large European study indicate that the outcome of primary hyperoxaluria type 1 correlates with the AGXT mutation type, Kidney Int. 86 (2014) 1197–1204, https://doi.org/10.1038/ki.2014.222.

[40] E. Oppici, R. Montioli, B. Cellini, Liver peroxisomal alanine:glyoxylate aminotransferase and the effects of mutations associated with primary hyperoxaluria type I: an overview, Biochim. Biophys. Acta 1854 (2015) 1212–1219, https://doi.org/10.1016/j.bbapap.2014.12.029.

[41] H. Cui, H. Shan, M.Z. Miao, Z. Jiang, Y. Meng, R. Chen, L. Zhang, Y. Liu, Identification of the key genes and pathways involved in the tumorigenesis and prognosis of kidney renal clear cell carcinoma, Sci. Rep. 10 (2020) 4271, https://doi.org/10.1038/s41598-020-61162-4.

[42] Y. Sun, W. Li, S. Shen, X. Yang, B. Lu, X. Zhang, P. Lu, Y. Shen, J. Ji, Loss of alanine-glyoxylate and serine-pyruvate aminotransferase expression accelerated the progression of hepatocellular carcinoma and predicted poor prognosis, J. Transl. Med. 17 (2019) 390, https://doi.org/10.1186/s12967-019-02138-5.

[43] C.L. Zhao, Y. Hui, L.J. Wang, D. Yang, E. Yakirevich, S. Mangray, C.K. Huang, S. Lu, Alanine-glyoxylate aminotransferase 1 (AGXT1) is a novel marker for hepatocellular carcinomas, Hum. Pathol. 80 (2018) 76–81, https://doi.org/10.1016/j.humpath.2018.05.025.

[44] X. Gao, L. Zhao, S. Liu, Y. Li, S. Xia, D. Chen, M. Wang, S. Wu, Q. Dai, H. Vu, L. Zacharias, R. DeBerardinis, E. Lim, C. Metallo, T.J. Boggon, S. Lonial, R. Lin, H. Mao, Y. Pan, C. Shan, J. Chen, Gamma-6-phosphogluconolactone, a byproduct of the oxidative pentose phosphate pathway, contributes to AMPK activation through Inhibition of PP2A, Mol. Cell 76 (2019) 857–871, https://doi.org/10.1016/j.molcel.2019.09.007, e859.

[45] H. Yadav, S. Devalaraja, S.T. Chung, S.G. Rane, TGF-beta1/Smad3 pathway targets PP2A-AMPK-FoxO1 signaling to regulate hepatic gluconeogenesis, J. Biol. Chem. 292 (2017) 3420–3432, https://doi.org/10.1074/jbc.M116.764910.

[46] P.A. Just, S. Charawi, R.G.P. Denis, M. Savall, M. Traore, M. Foretz, S. Bastu, S. Magassa, N. Senni, P. Sohier, M. Wursmer, M. Vasseur-Cognet, A. Schmitt, M. Le Gall, M. Leduc, F. Guillonneau, J.P. De Bandt, P. Mayeux, B. Romagnolo, S. Luquet, P. Bossard, C. Perret, Lkb1 suppresses amino acid-driven gluconeogenesis in the liver, Nat. Commun. 11 (2020) 6127, https://doi.org/10.1038/s41467-020-19490-6.

[47] J. Westermarck, B.G. Neel, Piecing together a broken tumor suppressor phosphatase for cancer therapy, Cell 181 (2020) 514–517, https://doi.org/10.1016/j.cell.2020.04.005.

[48] C.S. Hong, W. Ho, C. Zhang, C. Yang, J.B. Elder, Z. Zhuang, LB100, a small molecule inhibitor of PP2A with potent chemo- and radio-sensitizing potential, Cancer Biol. Ther. 16 (2015) 821–833, https://doi.org/10.1080/15384047.2015.1040961.

[49] C.L. Yang, X. Qiu, J.Y. Lin, X.Y. Chen, Y.M. Zhang, X.Y. Hu, J.H. Zhong, S. Tang, X. Y. Li, B.D. Xiang, Z.M. Zhang, Potential role and clinical value of PPP2CA in hepatocellular carcinoma, J. Clin. Transl. Hepatol. 9 (2021) 661–671, https://doi.org/10.14218/JCTH.2020.00168.

[50] F.H. Duong, M.T. Dill, M.S. Matter, Z. Makowska, D. Calabrese, T. Dietsche, S. Ketterer, L. Terracciano, M.H. Heim, Protein phosphatase 2A promotes hepatocellular carcinogenesis in the diethylnitrosamine mouse model through inhibition of p53, Carcinogenesis 35 (2014) 114–122, https://doi.org/10.1093/carcin/bgt258.

[51] S.J. Gong, X.J. Feng, W.H. Song, J.M. Chen, S.M. Wang, D.J. Xing, M.H. Zhu, S. H. Zhang, A.M. Xu, Upregulation of PP2Ac predicts poor prognosis and contributes to aggressiveness in hepatocellular carcinoma, Cancer Biol. Ther. 17 (2016) 151–162, https://doi.org/10.1080/15384047.2015.1121345.

[52] X.L. Bai, Q. Zhang, L.Y. Ye, Q.D. Hu, Q.H. Fu, X. Zhi, W. Su, R.G. Su, T. Ma, W. Chen, S.Z. Xie, C.L. Chen, T.B. Liang, Inhibition of protein phosphatase 2A enhances cytotoxicity and accessibility of chemotherapeutic drugs to hepatocellular carcinomas, Mol. Cancer Ther. 13 (2014) 2062–2072, https://doi.org/10.1158/1535-7163.MCT-13-0800.

[53] B. Sun, F.J. Zhong, C. Xu, Y.M. Li, Y.R. Zhao, M.M. Cao, L.Y. Yang, Programmed cell death 10 promotes metastasis and epithelial-mesenchymal transition of hepatocellular carcinoma via PP2Ac-mediated YAP activation, Cell Death. Dis. 12 (2021) 849, https://doi.org/10.1038/s41419-021-04139-z.